Graphical Abstract

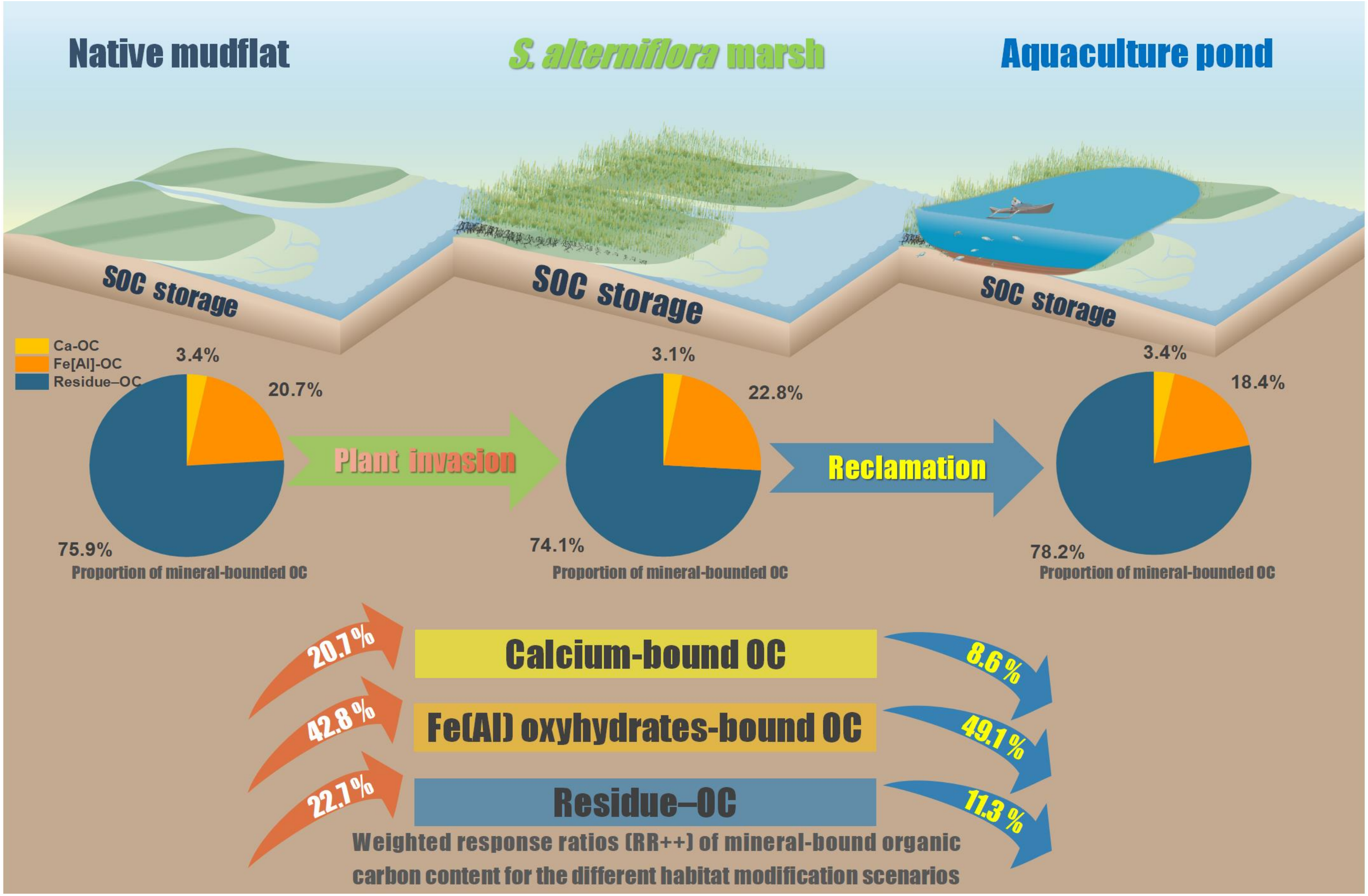

HIGHLIGHTS

- Invasion by *Spartina* increased mineral-bound OC in mudflat soil
- Subsequently reclamation for aquaculture decreased soil mineral-bound OC
- Mineral-bound OC was correlated to nitrogen supply and soil clay content
- Habitat change affected Fe[Al]-OC more than Ca-OC and residual-OC
- Soil OC storage increased more strongly with increasing Ca-OC

Variable responses of mineral-bound soil organic carbon to land cover change in southeastern China's coastal wetlands

Ping Yang[a,b,c], Guanpeng Chen[a], Linhai Zhang[a,c*], Chuan Tong[a,c], Hong Yang[d,e], Wanyi Zhu[a], Dongyao Sun[f*], Lishan Tan[g], Yan Hong[a], Kam W. Tang[h*]

[a]*School of Geographical Sciences, Fujian Normal University, Fuzhou 350117, P.R. China,*

[b]*Institute of Geography, Fujian Normal University, Fuzhou 350117, China*

[c]*Research Centre of Wetlands in Subtropical Region, Fujian Normal University, Fuzhou 350117, P.R. China*

[d]*Department of Geography and Environmental Science, University of Reading, Reading, UK*

[e]*College of Environmental Science and Engineering, Fujian Normal University, Fuzhou 350007, China*

[f]*School of Geography Science and Geomatics Engineering, Suzhou University of Science and Technology, Suzhou 215009, China*

[g]*Department of Geography and Resource Management, The Chinese University of Hong Kong, Shatin, New Territories, Hong Kong SAR, China*

[h]*Department of Biosciences, Swansea University, Swansea SA2 8PP, U. K.*

***Correspondence to:**

Linhai Zhang (mary12maryzhang@126.com); Dongyao Sun (dongyaos@126.com); Kam W. Tang (k.w.tang@swansea.ac.uk)

A B S T R A C T

The formation of mineral-bound organic carbon (OC) complexes is important for the long-term preservation of soil organic carbon (SOC) in wetlands. Many coastal wetlands globally are threatened by plant invasion and land development, but information on the effects on mineral-bound OC is limited. We measured the soil contents of Ca-OC, Fe(Al)-OC and residual OC across 21 coastal wetlands in southern China that have gone through the same sequence of land cover change, from native mudflats (MFs) to *Spartina alterniflora* marshes (SAs) then to earthen aquaculture ponds (APs). Residual-OC was the main component of SOC (74.1–78.2%), followed by Fe(Al)-OC (18.4–22.8%) and Ca-OC (<3.5%). All three components in the soil increased when MFs were converted to SAs, but decreased in subsequent conversion of SAs to APs. Land cover change affected Fe(Al)-OC the most, but SOC storage increased more strongly with increasing Ca-OC. Nitrogen supply in the form of NH_4^+-N and clay content both positively affected the changes in mineral-bound OC. Our results suggest that different land cover change scenarios had different effects on the amounts of mineral-bound OC and their liability to microbial turnover, resulting in different degrees of SOC preservation and carbon emission.

Keywords: Soil organic carbon stability; Mineral-bound OC; Chemical protection; Coastal wetland; Habitat change

1. Introduction

It is estimated that the global soil organic carbon (SOC) stock amounts to 1461×10^{15} gC (Scharlemann et al., 2014), which is more than double the atmospheric carbon pool (Friedlingstein et al., 2019). Accumulation and preservation of SOC is key to long-term sequestration of carbon (Gross and Harrison, 2019; Stockmann et al., 2013), and changes to SOC dynamics due to land development and land cover change (Li et al., 2022; Parras-Alcántara et al., 2016; Qiu et al., 2012) could have a large impact on atmospheric carbon dioxide level (Arneth et al., 2017; Leifeld et al., 2019; Zhong et al., 2019).

Wetlands represent 20–30 % of the global SOC inventory (Kayranli et al., 2010; Mitsch et al., 2013) and play a critical role in the carbon cycle (Were, et al., 2019; Zhu et al., 2020). While coastal wetlands (e.g., mangroves, salt marshes and seagrass meadows) cover <0.3 % of the ocean surface, their carbon burial rates are very high, at 44.6–53.7 Tg C yr^{-1} globally (Chmura et al., 2003; Wang et al., 2021a), contributing to approximately half of the carbon sequestered to the seafloor (Duarte et al., 2013). To achieve long-term sequestration, SOC must be exempt from microbial metabolism. Physical protection, chemical composition and interactions with minerals are all important factors for stabilizing OC in the soil (Giannetta et al., 2018; Liu et al., 2022; Wan et al., 2021). Coastal wetland soils contain large amounts of minerals and metal cations (e.g., Fe^{3+}, Al^{3+}, Ca^{2+}) compared to other habitats (Coelho et al., 2004; Kostka and Luther, 1994; Yu et al., 2021). These minerals can physically or chemically bind with OC to form mineral-bound OC complexes (Hu et al., 2023; Lalonde et al., 2012; Rowley et al., 2018), such as Ca-OC and Fe(Al)-OC. These mineral-bound OC complexes facilitate long-term SOC preservation by inhibiting microbial decomposition of the associated organic matter (Hemingway et al., 2019; Lin et al., 2023a; Schrumpf et al., 2013).

Over the last century, many coastal wetlands around the world have undergone degradation (Davidson et al., 2018; Fluet-Chouinard et al., 2023; Romañach et al., 2018) due to invasion by non-native species and land development (Lázaro-Lobo and Ervin, 2021; Newton et al., 2020; Tan et al., 2022). Coastal wetlands in mainland China span approximately ~57,900 km^2 (Sun et al., 2015), representing about 10% of its native wetland areas. Despite ongoing conservation effort (Mao et al., 2022), large swaths of native mudflats along the southeast coast have been taken over by the invasive *Spartina alterniflora* (Liu et al., 2018; Mao et al., 2019). To control this invasive species and to support food production, some of *S. alterniflora* marshes were subsequently cleared to create earthen aquaculture ponds (Duan et al. 2020; Meng et al., 2017; Wang et al., 2022). Recent estimates suggest that *S. alterniflora* marshes cover ~546 km^2 (Liu et al., 2018) and earthen aquaculture ponds cover ~15,600 km^2 (Duan et al., 2020), equivalent to a displacement of ~28% of the native wetland area. This extensive modification of the landscape could significantly change the soil properties (Meng et al., 2020; Wang et al., 2019; Yang et al., 2022a) and SOC contents (e.g., Hong et al., 2023; Tan et al., 2022; Xia et al., 2021), but relevant data on mineral-bound OC are lacking, which limits our understanding of changes in SOC preservation and storage.

In order to fill this knowledge gap, we studied the soil contents of mineral-bound OC (e.g., Ca-OC, Fe(Al)-OC) and residual-OC and soil physiochemical properties in 21 coastal wetlands in mainland China that have experienced the same sequence of land cover change, from native mudflats to *S. alterniflora* marshes then to earthen aquaculture pond. By comparing soil samples from the three habitat types within the same wetlands, we aimed to investigate the changing patterns of mineral-bound OC and key environmental drivers under different land cover change scenarios, and assess the importance of mineral-bound OC to SOC storage in these impacted coastal wetlands. We hypothesized that (1) invasion of mudflats by *S. alterniflora* would increase soil mineral-bound OC contents due to enhanced organic matter input from the marsh plants, and that (2) the change in soil mineral-bound OC contents would reverse when *S. alterniflora* marshes were cleared to create aquaculture ponds.

2. Materials and methods

2.1. Study areas

We selected 21 coastal wetlands across five provinces in China: Shanghai, Zhejiang, Fujian, Guangdong and Guangxi, covering a wide geographical range (20°42′ N to 31°51′ N, 109°11′ E to 122°11′ E; Figure 1). These provinces experience a tropical-subtropical monsoon climate, with annual average temperature of 11.0–23.0 ºC and rainfall ranging from 100 cm to 220 cm (Lin et al., 2023b; Yang et al., 2022a), and have a combined coastal wetland area of ~2.58×10^4 km^2 (Sun et al., 2015). In the past several decades, significant portions of their coastal mudflats were transformed into marshes by the invasive *S. alterniflora*. As a way to control the invasive species and to support food production, many of the *S. alterniflora* marshes were subsequently cleared to create earthen aquaculture ponds. Among these coastal provinces, *S. alterniflora* marshes and aquaculture ponds now cover approximately 334 km^2 and 5,309 km^2 (Liu et al., 2018; Duan et al., 2020), respectively.

2.2. Soil sampling and analysis

Field surveys and sampling were conducted in the three habitat types: native mudflats (MFs), *S. alterniflora* marshes (SAs) and aquaculture ponds (APs), within each of the 21 coastal wetlands between December 2019 and January 2020. In each of the MFs and SAs, three sampling sites were randomly selected. For each of the APs, one sampling site was near the bank of the pond, one at the center of the pond, and one at the mid-way point between the two. At each site, three replicate soil samples from the upper 20 cm were extracted using a steel corer of 5 cm diameter, then stored in sterile plastic bags. In total, 189 soil samples were collected (21 wetlands × 3 habitat types × 3 replicate plots) and immediately transported back to the laboratory in a cooler.

In the laboratory, portions of the soil samples were freeze-dried, then homogenized and ground into a fine powder for physicochemical characterization, including particle size distribution, water content, pH, salinity, ammonium-N (NH_4^+-N), nitrate-N (NO_3^--N), Cl^-, SO_4^{2-} and total SOC. Further details can be found in our companion studies (Hong et al., 2023; Lin et al., 2023b; Yang et al., 2022a; Yang et al., 2023). Here, we focused on the analysis of soil mineral-bound OC and its relationships with different physicochemical variables.

2.3. Determination of mineral-bound OC

Prior to determining mineral-bound OC, the mineral-associated organic matter (MaOM) was obtained using the method of Xu and Yuan (1993) and Yeasmin et al. (2017). Briefly, approximately 10 g of air-dried soil (sieved to <2 mm) and 30 mL of sodium polytungstate (SPT, density of 1.8 g cm^{-3}) solution were added to a 100 mL centrifuge tube. The tube was then shaken on a rotary shaker at 200 rpm and 25 °C for 3 h. Afterward, the tube was centrifuged at a speed of 4000 rpm for 10 min, and the resultant supernatant was filtered through a 0.7-μm glass fiber filter to obtain the particulate organic matter (POM). The residual solid material in the centrifuge tube was treated with an additional 30 mL of SPT solution, agitated for 1 h and centrifuged to obtain POM as before. This procedure was done for a total of three times to ensure complete extraction of free POM. The final residue in the centrifuge tube was subsequently rinsed with deionized water, then freeze-dried and ground for extracting MaOM as described next.

Ca-OC, Fe(Al)-OC and residual-OC in MaOM were obtained by a sequential extraction method adapted from Cui et al. (2014), Li et al. (2021a) and Wan et al. (2021). Briefly, 2 g of the MaOM sample and 20 mL of 0.5 M Na_2SO_4 solution (maintained at pH 7) were added to a 50 mL centrifuge tube. This mixture was agitated at 200 rpm and 25 °C for 2 h on a rotary shaker, left to settle overnight, and subsequently centrifuged at 4000 rpm for 15 min to separate Ca-OC. This extraction process was repeated until the extraction solution showed no presence of Ca. After washing with deionized water, the residue was treated with 20 mL mixture of 0.1 M $Na_4P_2O_7$ and 0.1 M NaOH solution to extract Fe(Al)-OC using the same procedures outlined above. The OC content of the extracts was determined with a TOC analyzer (Schimadzu TOC-$_{VCPH}$, Kyoto, Japan). Residual-OC was calculated by subtracting Ca-OC and Fe(Al)-OC from total SOC.

2.4. Statistical analysis

Latitudinal gradients of SOC components were tested by linear regressions. Significant differences in Ca-OC, Fe(Al)-OC, residual-OC and soil physicochemical properties among the habitat types were tested by analysis of variance (ANOVA) using the SPSS 25.0 software (IBM, Armonk, NY, USA). The relationship between Ca-OC, Fe(Al)-OC, residual-OC and soil physicochemical attributes were determined using Spearman's correlation analysis in the vegan package of R (version 4.1.0). To investigate how various soil physicochemical attributes affect the variability in Ca-OC, Fe(Al)-OC and residual-OC, redundancy analysis (RDA) was conducted using CANOCO 5.0 software (Microcomputer Power, Ithaca, USA). The indirect and direct effects of soil physicochemical properties on Ca-OC, Fe(Al)-OC and residual-OC under different land cover change scenarios were examined through structural equation modeling (SEM) in R Version 4.1.0, employing the lavaan package. Further insights into the SEM analysis are provided in Tan et al. (2022) and (2023). To assess the impact of habitat modification on Ca-OC, Fe(Al)-OC and residual-OC, weighted response ratios (RR_{++}) were computed following the method of Hedges et al. (1999) and Tan et al. (2020). A significance threshold of $p < 0.05$ was used for all analyses.

3. Results

3.1. Soil mineral-bound OC contents in different habitat types

Across all sites, Ca–OC concentrations varied in the range of 0.02–0.44 g kg^{-1} in MFs, 0.16–0.59 g kg^{-1} in SAs, and 0.02–0.55 g kg^{-1} in APs (Figure 2a). On average, Ca-OC content in SAs (0.31±0.01 g kg^{-1}) was significantly higher than that in MFs (0.24±0.02 g kg^{-1}), but comparable to APs (0.27±0.02 g kg^{-1}) (Figure 2a).

Fe(Al)–OC content showed marked variations across habitat types: 0.16–4.64 g kg^{-1} in MFs, 0.38–5.90 g kg^{-1} in SAs, and 0.40–20.67 g kg^{-1} in APs (Figure 2b). The average value was significantly higher in SAs (2.38 ± 0.37 g kg^{-1}), but was comparable between MFs (1.52 ± 0.25 g kg^{-1}) and APs (1.49 ± 0.24 g kg) (Figure 2b).

Residual–OC content varied in the range of 1.36–15.89 g kg^{-1} in MFs, 3.04–21.51 g kg^{-1} in SAs, and 1.06–4.89 g kg^{-1} in APs (Figure 2c). The average value was 7.71 ± 0.85 g kg^{-1} in SAs, which was significantly higher than that in MFs (5.58 ± 0.68 g kg^{-1}), but comparable to APs (6.28 ± 0.81 g kg^{-1}) (Figure 2c).

3.2. Effects of different land cover change scenarios

Across all samples, SOC storage increased linearly with the bound organic carbon contents in the top soil (p<0.01), and the relationship was strongest for Ca–OC, followed by Fe(Al)–OC and residual-OC (Figure 3). Overall, residual–OC accounted for the majority of bound OC (74.1–78.2%), followed by Fe(Al)–OC (18.4–22.8%) and Ca–OC (3.1–3.4%) (Figure 4).

We used weighted RR analysis to assess the effects of different land cover change scenarios on mineral-bound OC contents. In the case of land cover change from MFs to SAs, Ca–OC concentration increased by approximately 20.7% (Figure 5a), Fe(Al)–OC content increased by 42.8% (Figure 5b), and residual–OC increased by 22.7% (Figure 5c). When SAs were subsequently cleared and converted to APs, Ca–OC concentration decreased by 8.6% (Figure 5a), Fe(Al)–OC content decreased by 49.1% (Figure 5b), and residual–OC decreased by 11.3% (Figure 5c).

3.3. Environmental control of mineral-bound OC and SOC

There were significant and negative latitudinal gradients of Ca-OC and residual-OC concentrations, and a positive latitudinal gradient of Fe(Al)-OC concentration (Figure 6).

Based on Spearman correlation (Figure 7) and RDA (Figure 8) analyses, soil NH_4^+-N was the strongest factor driving the change in mineral-bound OC and SOC contents in both MFs-to-SAs and SAs-to-APs land cover change scenarios. The other key factors included pH, clay and Fe(III) in MFs-to-SAs conversion scenario (Figure 8a); Fe(III), sand and clay in SAs-to-APs conversion scenarios (Figure 8b).

The PLS-SEM analysis results indicated that NH_4^+-N had a positive and direct effect on Ca-OC, residual-OC and SOC storage in both land cover change scenarios (Figures 9a, c, d, f), and a negative effect on Fe(Al)-OC in the transformation from SAs to APs (Figures 9e). Both Fe(III) and clay had positive direct effects on Ca-OC (Figure 9a, d), Fe(Al)-OC (Figure 9b, e) and residual-OC (Figure 9f). Clay positively affected Ca-OC (Figure 9a, d) and Fe(Al)-OC (Figure 9b, e). In addition, land cover change affected SOC storage by changing pH (Figure 9b, d, e, f) and mineral-bound OC contents.

4. Discussion

4.1. Mineral-bound OC in different habitat types

Across the broad geographical range, we observed a negative latitudinal gradient in Ca-OC contents (Figure 6). Soils at higher latitudes tend to receive less precipitation, leading to lower contents of exchangeable Ca^{2+} in the soil (Li et al., 2023), which likely limit the formation of Ca-OC. We also observed a negative latitudinal gradient in residual-OC (Figure 6). The warmer and wetter climate at the lower latitudes may have increased biological productivity and subsequent deposition of organic matter into the soil, as supported by the latitudinal gradient in SOC content observed along China's coast (Hong et al., 2023), which may then increase the amount of residual-OC. In contrast, Fe(Al)-OC was less in the lower latitudes (Figure 6), which perhaps was due to the warmer and wetter soil conditions promoting the conversion of Fe(III) to Fe(II) and its subsequent loss from the soil (Chari et al., 2021). Nevertheless, it should be noted the r-squared values of these relationships were low (0.10-0.32), meaning that their effects on mineral-bound OC were overall rather weak.

Mineral-associated OC is often the dominant fraction of the SOC pool, accounting for 50–80 % of SOC (Cotrufo et al., 2019), and many studies have highlighted the importance of physical and chemical interactions between OC with minerals in sequestering and preserving SOC in terrestrial ecosystems (Hemingway et al., 2019; Lalonde et al., 2012; Lv et al., 2023; Schrumpf et al., 2013). Based on soil samples from the 21 coastal wetlands, the proportion of Ca–OC in our research areas was 3.1–3.4% (Figure 4). This was considerably lower than farmed soils (e.g. Wan et al., 2021; Wei et al., 2017), suggesting that calcium contained in fertilizers would enhance Ca-OC formation. Our values were also lower than that observed in mangrove wetland (Wang et al., 2021b) and delta (Li et al., 2021a), perhaps reflecting the overall weak seawater influence in our sampling sites (salinity <5 ‰; Yang et al., 2022a). In comparison, Fe(Al)–OC constituted a larger fraction of SOC in the three habitat types (18.4–22.8%; Figure 4), which fell within the range observed in other terrestrial ecosystems (15%–38%; Lalonde et al., 2012; Faust et al., 2021; Shields et al., 2016; Zhao et al., 2023), suggesting comparable availability and reactivity of Fe/Al between terrestrial and coastal soils.

4.2. Response of mineral-bound OC to habitat changes

Our results showed that coastal land cover change had notable impacts on mineral-bound OC. Invasion of native mudflats by *S. alterniflora* boosted the contents of Ca-OC, Fe(Al)-OC and residual-OC by 20.7–42.8%, whereas transforming these *S.*

alterniflora marshes into aquaculture ponds decreased them by 8.6–49.1% (Figure 2). This might be attributed to the change in vegetation coverage and hydrology following habitat modification. Plants are a main source of OC (Mcleod et al., 2011) and a key factor affecting the accumulation of OC and mineral in coastal wetlands (Bai et al., 2021; Cragg et al., 2020). In general, persistent river flow and regular tidal flushing in non-vegetated mudflats enhance soil erosion and minimize OC deposition (Hong et al., 2023). In the 1980s, the exotic *S. alterniflora* was introduced to China to mitigate soil erosion, with its aboveground biomass slowing the water flow (Yang et al., 2023; Zhang et al., 2021) and its subterranean roots stabilizing the soil (Hsieh et al., 2021; Li et al., 2021b), which would retain more OC and mineral and allow for the formation of mineral-bound OC. Furthermore, *S. alterniflora* invasion would result in higher soil water content, which has been linked to enhanced anoxic condition that fosters the formation of Fe-OC (Hu et al., 2023; Song et al., 2022; Yu et al., 2021). However, removing *S. alterniflora* to construct earthen aquaculture ponds would eliminate the input of plant-derived organics to the soil. Furthermore, the common practice of pond drainage and drying between farming seasons would lead to further reduction in OC and minerals in the ponds (Alongi et al., 2000; Kauffman et al., 2018; Yang et al., 2022b). These factors likely contributed to the lower Ca-OC, Fe(Al)-OC and residual-OC contents in aquaculture ponds relative to *S. alterniflora* marshes (Figure 2).

4.3. Effects of nitrogen and soil texture on mineral-bound OC

Our correlation and SEM analyses showed that nitrogen supply strongly affected the change in Ca-OC and residual-OC contents (Figures 7 and 9), which reflects the nitrogen-limiting condition in these coastal wetlands and the effects of vegetation in increasing soil N contents (Feng et al., 2017; Jia et al., 2017), which would be conducive to the production of organic carbon by both plants and microbes (Xie et al., 2019; Pastore et al., 2017). The encroachment of native mudflats by *S. alterniflora* significantly increased the soil NH_4^+-N content (Yang et al., 2023), likely due to nitrogen remineralization and retention by *S. alterniflora* biomass (Liao et al., 2007). Conversely, removal of *S. alterniflora* for the development of aquaculture ponds resulted in opposite changes (Figure 5).

Soil texture can also affect the preservation of SOC (Gonçalves et al., 2017; Singh et al., 2018). Compared to sand and silt, clay particles have smaller pores, higher surface area-to-volume ratio and more binding sites (Giannetta et al., 2019; Riedel and Weber, 2016; Ye et al., 2017), which could facilitate the formation of microaggregate structures (Lehmann et al., 2007; Totsche et al., 2017) that effectively decrease microbial breakdown of organic matter (Ransom et al., 1998; Yu et al., 2019). As a result, clay associated carbon can be adsorbed by minerals more effectively (Hu et al., 2023; Ye et al., 2017; Fang et al., 2019). In our study areas, the transformation of native mudflats to *S. alterniflora* marshes resulted in a 5.1% increase in soil clay content, while subsequent conversion to aquaculture ponds led to a 4.1% reduction (Yang et al., 2022a). Accordingly, clay content was a significant factor in the changes in mineral-bound OC (Figures 8 and 9), similar to the observations by others (Fang et al., 2019; Hu et al., 2023; Zhao et al., 2023).

4.4. Land cover change effects on SOC accumulation and preservation

In recent decades, China's coastal regions have experienced significant changes due to *S. alterniflora* invasion (Liu et al., 2018; Mao et al., 2019) and aquaculture development (Duan et al. 2020; Wang et al., 2022), which has significantly changed the size of SOC pool and SOC mineralization rate (Yang et al., 2022a). Given the importance of mineral-bound OC in preserving SOC, it is imperative to investigate how mineral-bound OC responds to land cover change in coastal wetlands.

Overall, SOC storage increased more strongly with increasing Ca–OC content than Fe(Al)–OC and residual–OC (Figure 3), suggesting that Ca–OC may play a more vital role in preserving and sequestering SOC in these coastal wetlands. Because the proportion of Ca-OC decreased when mudflats were transformed into *S. alterniflora* marshes and it increased when these marshes were later converted into aquaculture ponds, we may expect that SOC preservation and sequestration would also decrease and increase accordingly. This is consistent with our earlier observations that *S. alterniflora* invasion of mudflats increased the liability and microbial turnover of SOC (Yang et al., 2022a). Overall, while *S. alterniflora* invasion would increase the total SOC, it would also compromise the stability and preservation of wetland SOC, similar to others' findings (Lin et al., 2023a; Xia et al., 2021; Zhang et al., 2021).

5. Conclusions

This study, in conjunction with related research, revealed that land cover change had significant impacts on soil organic carbon in coastal wetlands across a wide geographical range in southeastern China. Consistent with our hypothesis, the invasion of native mudflats by *S. alterniflora* led to an increase in both mineral-bound OC and total SOC (this study; Hong et al., 2023), but the liability and microbial turnover of SOC also increased, resulting in a lower degree of SOC preservation and higher carbon greenhouse gas emissions (Yang et al., 2022a). Conversely, the conversion of *S. alterniflora* marshes into aquaculture ponds reversed these effects. Therefore, different land cover change scenarios resulted in different SOC dynamics partly by altering the mineral-bound OC fractions in the soil.

Declaration of competing interest

The authors declare that they have no known competing financial interests or personal relationships that could have appeared to influence the work reported in this paper.

Acknowledgements

The study was funded by the Natural Science Foundation of Fujian Province (No. 2021J01178, 2022R1002006), the National Science Foundation of China (No. 41801070, 41671088), and the Minjiang Scholar Programme.

References

Alongi, D.M., Johnston, D.J., Xuan, T.T., 2000. Carbon and nitrogen budgets in shrimp ponds of extensive mixed shrimp–mangrove forestry farms in the Mekong Delta, Vietnam. Aquac. Res. 31, 387–399.

Arneth, A., Sitch, S., Pongratz, J., Stocker, B.D., Ciais, P., Poulter, B., Bayer, A.D., Bondeau, A., Calle, L., Chini, L.P., Gasser, T., Fader, M., Friedlingstein, P., Kato, E., Li, W., Lindeskog, M., Nabel, J.E.M.S., Pugh, T.A.M., Robertson, E., Viovy, N., Yue, C., Zaehle, S., 2017. Historical carbon dioxide emissions caused by land-use changes are possibly larger than assumed. Nat. Geosci. 10(2), 79-84. 17 | https://doi.org/10.1038/NGEO2882.

Chari, N.R., Lin, Y., Lin, Y.S., Silver, W.L., 2021. Interactive effects of temperature and redox on soil carbon and iron cycling. Soil Biol. Biochem. 157, 108235. https://doi.org/10.1016/j.soilbio.2021.108235.

Chmura, G.L., Anisfeld, S.C., Cahoon, D.R., Lynch, J.C., 2003. Global carbon sequestration in tidal, saline wetland soils. Global Biogeochem. Cy. 17(4), 1111. https://doi.org/10.1029/2002GB001917.

Coelho, J.P., Flindt, M.R., Jensen, H.S., Lillebø, A.I., Pardal, M.Â., 2004. Phosphorus speciation and availability in intertidal sediments of a temperate estuary: relation to eutrophication and annual P-fluxes. Estuar. Coast. Shelf S. 61(4), 583–590. https://doi.org/10.1016/j.ecss.2004.07.001.

Cotrufo, M.F., Ranalli, M.G., Haddix, M.L., Six, J., Lugato, E., 2019. Soil carbon storage informed by particulate and mineral-associated organic matter. Nat. Geosci. 12, 989–994. https://doi.org/10.1038/s41561-019-0484-6.

Cragg, S.M., Friess, D.A., Gillis, L.G., Trevathan-Tackett, S.M., Terrett, O.M., Watts, J.E., Distel, D.L., Dupree, P., 2020. Vascular plants are globally significant contributors to marine carbon fluxes and sinks. Annu. Rev. Mar. Sci. 12, 469–497. https://doi.org/10.1146/annurev-marine-010318-095333.

Cui, J., Li, Z.X., Liu, Z.T., Ge, B.M., Fang, C.M., Zhou, C.L., Tang, B.P., 2014. Physical and chemical stabilization of soil organic carbon along a 500-year cultived soil chronosequence originating from estuarine wetlands: temporal patterns and land use effects. Agr. Ecosyste. Environ. 196, 10–20.

http://dx.doi.org/10.1016/j.agee.2014.06.013.

Davidson, N.C., Fluet-Chouinard, E., Finlayson, C.M., 2018. Global extent and distribution of wetlands: trends and issues. Mar. Freshwater Res. 69, 620–627. https://doi.org/10.1071/MF17019.

Duan, Y.Q., Li, X., Zhang, L.P., Chen, D., Liu, S.A., Ji, H.Y., 2020. Mapping national-scale aquaculture ponds based on the Google Earth Engine in the Chinese coastal zone. Aquaculture 520, 734666. https://doi.org/10.1016/j.aquaculture.2019.734666.

Duarte, C.N., Losada, I.J., Hendriks, I.E., Mazarrasa, I., Marbà, N., 2013. The role of coastal plant communities for climate change mitigation and adaptation. Nat. Clim. Change 3 (11), 961–968. https://doi.org/10.1038/nclimate1970.

Fang, K., Qin, S.Q., Chen, L.L., Zhang, Q.W., Yang, Y.H., 2019. Al/Fe mineral controls on soil organic carbon stock across tibetan alpine grasslands. J. Geophys. Res-Biogeo. 124, 247–259. https://doi.org/10.1029/2018JG004782.

Faust, J.C., Tessin, A., Fisher, B.J., Zindorf, M., Papadaki, S., Hendry, K. R., Doyle, K. A., and Marz, C., 2021. Millennial scale persistence of organic carbon bound to iron in Arctic marine sediments. Nat. Commun. 12, 275. https://doi.org/10.1038/s41467-020-20550-0.

Feng, J.X., Zhou, J., Wang, L.M., Cui, X.W., Ning, C.X., Wu, H., Zhu, X.S., Lin, G., 2017. Effects of short-term invasion of *Spartina alterniflora* and the subsequent restoration of native mangroves on the soil organic carbon, nitrogen and phosphorus stock. Chemosphere 184, 774–783. https://doi.org/10.1016/j.chemosphere.2017.06.060.

Fluet-Chouinard, E., Stocker, B.D., Zhang, Z., Malhotra, A., Melton, J.R., Poulter, B., Kaplan, J.O., Goldewijk, K.K., Siebert, S., Minayeva, T., Hugelius, G., Joosten, H., Barthelmes, A., Prigent, C., Aires, F., Hoyt, A.M., Davidson, N., Finlayson, C.M., Lehner, B., Jackson, R.B., McIntyre, P.B., 2023. Extensive global wetland loss over the past three centuries. Nature 614, 281–286.

https://doi.org/10.1038/s41586-022-05572-6.

Friedlingstein, P., Jones, M.W., O'Sullivan, M., Andrew, R.M., Hauck, J., Peters, G.P., Peters, W., Pongratz, J., Sitch, S., Quéré, C.L., Bakker, D.C.E., Canadell, J.G., et al. 2019. Global Carbon Budget 2019. Earth Syst. Sci. Data 2019, 11, 1783–1838. https://doi.org/10.5194/essd-11-1783-2019.

Giannetta, B., Plaza, C., Vischetti, C., Cotrufo, M.F., Zaccone, C., 2018. Distribution and thermal stability of physically and chemically protected organic matter fractions in soils across different ecosystems. Biol. Fert. Soils 54, 671–681. https://doi.org/10.1007/s00374-018-1290-9.

Gonçalves, D.R.P., Sá, J.C., Mishra, U., Cerri, C.E.P., Ferreira, L.A., Furlan, F.J.F., 2017. Soil type and texture impacts on soil organic carbon storage in a sub-tropical agro-ecosystem. Geoderma 286, 88–97. https://doi.org/10.1016/j.geoderma.2016.10.021.

Gross, C.D., Harrison, R.B., 2019. The case for digging deeper: soil organic carbon storage, dynamics, and controls in our changing world. Soil Systems, 3(2), 28. https://doi.org/10.3390/soilsystems3020028.

Hedges, L.V., Gurevitch, J., Curtis, P.S., 1999. The meta-analysis of response ratios in experimental ecology. Ecology 80, 1150-1156. https://doi.org/10.2307/177062.

Hemingway, J.D., Rothman, D.H., Grant, K.E., Rosengard, S.Z., Eglinton, T.I., Derry, L.A., Galy, V.V., 2019. Mineral protection regulates long-term global preservation of natural organic carbon. Nature 570(7760), 228-231. https://doi.org/10.1038/s41586-019-1280-6.

Hong, Y., Zhang, L.H., Yang, P., Tong, C., Lin, Y.X., Lai, D.Y. F., Yang, H., Tian, Y.L., Zhu, W.Y., Tang, K.W., 2023. Responses of coastal sediment organic and inorganic carbon to habitat modification across a wide latitudinal range in southeastern China. Catena 225, 107034. https://doi.org/10.1016/j.catena.2023.107034.

Hsieh, S.-H., Yuan, C.-S., Ie, I.-R., Yang, L., Lin, H.-J., Hsueh, M.-L., 2021. In-situ measurement of greenhouse gas emissions from a coastal estuarine wetland using a novel continuous monitoring technology: comparison of indigenous and exotic plant species. J. Environ. Manage. 281, 111905 https://doi.org/10.1016/j.jenvman.2020.111905.

Hu, D.H., Lan, W.J., Luo, M., Fan, T.N., Chen, X., Tan, J., Li, S.H., Guo, P.P., Huang, J.F., 2023. Increase in iron-bound organic carbon content under simulated sea-level rise: A "marsh organ" field experiment. Soil Biol. Biochem. 187, 109217. https://doi.org/10.1016/j.soilbio.2023.109217.

Jia, J, Bai, J.H., Gao, H.F., Wen, X.J., Zhang, G.L., Cui, B.S., Liu, X.H., 2017. In situ soil net nitrogen mineralization in coastal salt marshes (*Suaeda salsa*) with different flooding periods in a Chinese estuary. Ecol. Indic. 73, 559–565. https://doi.org/10.1016/j.ecolind.2016.10.012.

Kauffman, J.B., Bernardino, A.F., Ferreira, T.O., Bolton, N.W., Gomes, L.E.O., Nobrega, G.N., 2018. Shrimp ponds lead to massive loss of soil carbon and greenhouse gas emissions in northeastern Brazilian mangroves. Ecol. Evol. 8, 5530–5540. https://doi.org/10.1002/ece3.4079.

Kayranli, B., Scholz, M., Mustafa, A., Hedmark, Å., 2010. Carbon storage and fluxes within freshwater wetlands: A critical review. Wetlands 30(1), 111–124. https://doi.org/10.1007/s13157-009-0003-4.

Kostka, J.E., Luther III, G.W., 1994. Partitioning and speciation of solid phase iron in saltmarsh sediments. Geochim. Cosmochim. Ac. 58, 1701–1710. https://doi.org/10.1016/0016-7037(94)90531-2.

Lalonde, K., Mucci, A., Ouellet, A., Gélinas, Y., 2012. Preservation of organic matter in sediments promoted by iron. Nature 483, 198–200. https://doi.org/10.1038/nature10855.

Lázaro-Lobo, A., Ervin, G. N.,2021. Wetland invasion: a multi-faceted challenge during a time of rapid global change. Wetlands, 41(5), 64. https://doi.org/10.1007/s13157-021-01462-1.

Lehmann, J., Kinyangi, J., Solomon, D., 2007. Organic matter stabilization in soil microaggregates: implications from spatial heterogeneity of organic carbon contents and carbon forms. Biogeochemistry 85, 45–57. https://doi.org/10.1007/s10533-007-9105-3.

Leifeld, J., Wüst-Galley, C., Page, S., 2019. Intact and managed peatland soils as a source and sink of GHGs from 1850 to 2100. Nature Climate Change 9, 945–947. https://doi.org/10.1038/s41558-019-0615-5.

Li, X.J., Yang, T.H., Hicks, L.C., Hu, B., Li, F.L., Liu, X., Wei, D.D., Wang, Z.L., Bao, W.K. 2023. Climate and soil properties drive soil organic and inorganic carbon patterns across a latitudinal gradient in southwestern China. J Soils Sediments 23, 91–102. https://doi.org/10.1007/s11368-022-03308-7.

Li, Y., Fu, C.C., Zeng, L., Zhou, Q., Zhang, H.B., Tu, C., Li, L.Z., Luo, Y.M., 2021a. Changes in organic carbon fractions and sources in deltaic topsoil and subsoil layers: autochthonous and allochthonous inputs. Eur. J. Soil Sci. 72(5), 2276–2291. https://doi.org/10.1111/ejss.13109.

Li, S.H., Ge, Z.M., Tan, L.S., Zhou, K., Hu, Z.J., 2021b. Coupling *Scirpus* recruitment with *Spartina* control guarantees recolonization of native sedges in coastal wetlands. Ecol. Eng. 166, 106246. https://doi.org/10.1016/j.ecoleng.2021.106246.

Li, Y.G., Liu, W., Feng, Q., Zhu, M., Yang, L.S., Zhang, J.T., 2022. Effects of land use and land cover change on soil organic carbon storage in the Hexi regions, Northwest China. J. Environ. Manage. 312, 114911. https://doi.org/10.1016/j.jenvman.2022.114911.

Liao, C.Z., Luo, Y.Q., Jiang, L.F., Zhou, X.H., Wu, X.W., Fang, C.M., Chen, J.K., Li, B., 2007. Invasion of *Spartina alterniflora* enhanced ecosystem carbon and nitrogen stocks in the Yangtze Estuary, China. Ecosystems 10, 1351–1361. https://doi.org/10.1007/s10021-007-9103-2.

Lin, M.F., Chen, Y., Cheng, L.W., Zheng, Y., Wang, W.Q., Sardans, J., Song, Z.L., Guggenberger, G., Zou, Y.C., Ding, X.L., Tariq, A., Zeng, F.J., Alrefaei, A.F., Peñuelas, J., 2023a. Response of topsoil Fe-bound organic carbon pool and microbial community to *Spartina alterniflora* invasion in coastal wetlands. Catena 232, 107414. https://doi.org/10.1016/j.catena.2023.107414.

Lin, X., Yang, Y.L., Yang, P., Hong, Y., Zhang, L.H., Tong, C., Lai, D.Y.F., Lin, Y.X., Tan, L.S., Tian, Y.L., Tang, K.W., 2023b. Soil organic nitrogen content and composition in different wetland habitat types along the south-east coast of China. Catena 232, 107457. https://doi.org/10.1016/j.catena.2023.107457.

Liu, M.Y., Mao, D.H., Wang, Z.M., Li, L., Man, W.D., Jia, M.M., Ren, C.Y., Zhang, Y.Z., 2018. Rapid invasion of *Spartina alterniflora* in the coastal zone of mainland China: new observations from landsat OLI images. Remote Sensing 10, 1933. https://doi.org/10.3390/rs10121933.

Liu, X.Y., Wang, W.Q., Peñuelas, J., Sardans, J., Chen, X.X., Fang, Y.Y., Alrefaei, A.F., Zeng, F.J., Tariq, A., 2022. Effects of nitrogen-enriched biochar on subtropical paddy soil organic carbon pool dynamics. Sci. Total Environ. 851, 158322. http://dx.doi.org/10.1016/j.scitotenv.2022.158322.

Lv, J.F., Shi, J., Wang, Z., Peng, Y.M., Wang, X., 2023. Effects of erosion and deposition on the extent and characteristics of organic carbon associated with soil minerals in Mollisol landscape. Catena 228, 107190. https://doi.org/10.1016/j.catena.2023.107190.

Mao, D.H., Liu, M.Y., Wang, Z.M., Li, L., Man, W.D., Jia, M.M., Zhang, Y.Z., 2019. Rapid invasion of *Spartina alterniflora* in the coastal zone of mainland China: spatiotemporal patterns and human prevention. Sensors 19, 2308. https://doi.org/10.3390/s19102308.

Mao, D.H., Yang, H., Wang, Z.M., Song, K.S., Thompson, J.R., 2022. Reverse the hidden loss of China's wetlands. Science, 376(6597), 1061–1061. https://doi.org/10.1126/science.adc8833.

Mcleod, E., Chmura, G.L., Bouillon, S., Salm, R., Bjork, ̈ M., Duarte, C.M., Lovelock, C.E., Schlesinger, W.S., Silliman, B.R., 2011. A blueprint for blue carbon: toward an improved understanding of the role of vegetated coastal habitats in sequestering

CO_2. Front. Ecol. Environ. 9, 552–560. https://doi.org/10.1890/110004.

Meng, W.Q., He, M.X., Hu, B.B., Mo, X.Q., Li, H.Y., Liu, B.Q., Wang, Z., 2017. Status of wetlands in China: A review of extent, degradation, issues and recommendations for improvement. Ocean Coast. Manage. 146, 50–59. https://doi.org/10.1016/j.ocecoaman.2017.06.003.

Meng, W.Q., Feagin, R.A., Innocenti, R.A., Hu, B.B.,, He, M.X., Li, H.Y., 2020. Invasion and ecological effects of exotic smooth cordgrass *Spartina alterniflora* in China. Ecol. Eng. 143, 105670. https://doi.org/10.1016/j.ecoleng.2019.105670.

Mitsch, W.J., Bernal, B., Nahlik, A.M., Mander, Ü., Zhang, L., Anderson, C.J., Jørgensen, S.E., Brix, H., 2013. Wetlands, carbon, and climate change. Landscape Ecol. 28(4), 583–597. https://doi.org/10.1007/s10980-012-9758-8.

Newton, A., Icely, J., Cristina, S., Perillo, G.M., Turner, R.E., Ashan, D., Cragg, S., Luo, Y.M., Tu, C., Li, Y., Zhang, H.B., Ramesh, R., Forbes, D.L., Solidoro, C., Béjaoui, B., Gao, S., Pastres, R., Kelsey, H., Taillie, D., Nhan, N., Brito, A.C., de Lima, R., Kuenzer, C., 2020. Anthropogenic, direct pressures on coastal wetlands. Front. Ecol. Evol. 8, 144. https://doi.org/10.3389/fevo.2020.00144.

Parras-Alcántara, L., Lozano-García, B., Keesstra, S., Cerd` a, A., Brevik, E.C., 2016. Longterm effects of soil management on ecosystem services and soil loss estimation in olive grove top soils. Sci. Total Environ. 571, 498–506. https://doi.org/10.1016/j.scitotenv.2016.07.016.

Pastore, M.A., Megonigal, J.P., Langley, J.A., 2017. Elevated CO_2 and nitrogen addition accelerate net carbon gain in a brackish marsh. Biogeochemistry 133, 73–87. https://doi.org/10.1007/s10533-017-0312-2.

Qiu, L.P., Wei, X.R., Zhang, X.C., Cheng, J.M., Gale, W.J., Guo, C., Long, T., 2012. Soil organic carbon losses due to land use change in a semiarid grassland. Plant Soil, 355, 299–309. https://doi.org/10.1007/s11104-011-1099-x.

Ransom, B., Kim, D., Kastner, M., Wainwright, S., 1998. Organic matter preservation on continental slopes: Importance of mineralogy and surface area. Geochim.

Cosmochim. Ac. 62(8), 1329–1345. https://doi.org/10.1016/S0016-7037(98)00050-7.

Riedel, T., Weber, T.K., 2016. The chemical potential of water in soils and sediments. Soil Sci. Soc. Am. J. 80, 79–83. https://doi.org/10.2136/sssaj2015.02.0085.

Romañach, S.S., DeAngelis, D.L., Koh, H.L., Li, Y.H., Teh, S.Y., Barizan, R.S.R., Zhai, L., 2018. Conservation and restoration of mangroves: Global status, perspectives, and prognosis. Ocean Coast. Manage. 154, 72–82. https://doi.org/10.1016/j.ocecoaman.2018.01.009.

Rowley, M.C., Grand, S., Verrecchia, É.P., 2018. Calcium-mediated stabilisation of soil organic carbon. Biogeochemistry 137, 27–49. https://doi.org/10.1007/s10533-017-0410-1.

Scharlemann, J.P., Tanner, E.V., Hiederer, R., Kapos, V., 2014. Global soil carbon: understanding and managing the largest terrestrial carbon pool. Carbon Manag. 5(1), 81–91. https://doi.org/10.4155/cmt.13.77.

Schrumpf, M., Kaiser, K., Guggenberger, G., Persson, T., Kögel-Knabner, I., Schulze, E.D., 2013. Storage and stability of organic carbon in soils as related to depth, occlusion within aggregates, and attachment to minerals. Biogeosciences, 10(3), 1675–1691. https://doi.org/10.5194/bg-10-1675-2013.

Shields, M.R., Bianchi, T.S., Gélinas, Y., Allison, M.A., Twilley, R.R., 2016. Enhanced terrestrial carbon preservation promoted by reactive iron in deltaic sediments. Geophys. Res. Lett. 43(3), 1149–1157. https://doi.org/10.1002/2015gl067388.

Singh, M., Sarkar, B., Sarkar, S., Churchman, J., Bolan, N., Mandal, S., Menon, M., Purakayastha, T.J., Beerling, D.J., 2018. Stabilization of soil organic carbon as influenced by clay mineralogy. Adv. Agron. 148, 33–84. https://doi.org/10.1016/bs.agron.2017.11.001.

Song, X.X., Wang, P., Van Zwieten, L., Bolan, N., Wang, H.L., Li, X.M., Cheng, K., Yang, Y., Wang, M.L., Liu, T.X., Li, F.B., 2022. Towards a better understanding of the role of Fe cycling in soil for carbon stabilization and degradation. Carbon Res. 1,

5. https://doi.org/10.1007/s44246-022-00008-2.

Stockmann, U., Adams, M.A., Crawford, J.W., Field, D.J., Henakaarchchi, N., Jenkins, M., Minasny, B., McBratney, A.B., de Remy de Courcelles, V., Singh, K., Wheeler, I., Abbott, L., Angers, D.A., Baldock, J., Bird, M., Brookes, P.C., Chenu, C., Jastrow, J.D., Lal, R., Lehmann, J., O'Donnell, A.G., Parton, W.J., Whitehead, D., Zimmermann, M., 2013. The knowns, known unknowns and unknowns of sequestration of soil organic carbon. Agr. Ecosyst. Environ. 164, 80-99. http://dx.doi.org/10.1016/j.agee.2012.10.001.

Sun, Z.G., Sun, W.G., Tong, C., Zeng, C.S., Yu, X., Mou, X.J., 2015. China's coastal wetlands: Conservation history, implementation efforts, existing issues and strategies for future improvement. Environ. Int. 79, 25–41. https://doi.org/10.1016/j.envint.2015.02.017.

Tan, L.S., Ge, Z.M., Zhou, X.H., Li, S.H., Li, X.Z., Tang, J.W., 2020. Conversion of coastal wetlands, riparian wetlands, and peatlands increases greenhouse gas emissions: A global meta-analysis. Global Change Biol. 26, 1638–1653. https://doi.org/10.1111/gcb.14933.

Tan, L.S., Ge, Z.M., Ji, Y.H., Lai, D.Y.F., Temmerman, S., Li, S.H., Li, X.Z., Tang, J.W., 2022. Land use and land cover changes in coastal and inland wetlands cause soil carbon and nitrogen loss. Global Ecol. Biogeogr. 31, 2541-2563. https://doi.org/10.1111/geb.13597.

Tan, L.S., Zhang, L.H., Yang, P., Tong, C., Lai, D.Y.F., Yang, H., Hong, Y., Tian, Y.L., Tang, C., Ruan, M.J., Tang, K.W., 2023. Effects of conversion of coastal marshes to aquaculture ponds on sediment anaerobic CO_2 production and emission in a subtropical estuary of China. J. Environ. Manage. 338, 117813. https://doi.org/10.1016/j.jenvman.2023.117813.

Totsche, K.U., Amelung, W., Gerzabek, M.H., Guggenberger, G., Klumpp, E., Knief, C., Lehndorff, E., Mikutta, R., Peth, S., Prechtel, A., Ray, N., Kogel-Knabner, ̈ I., 2017. Microaggregates in soils. J. Plant Nutr. Soil Sci. 181, 104–136.

https://doi.org/10.1002/jpln.201600451.

Wan, D., Ma, M.K., Peng, N., Luo, X.S., Chen, W.L., Cai, P., Wu, L.H., Pan, H.B., Chen, J.B., Yu, G.H., Huang, Q.Y., 2021. Effects of long-term fertilization on calcium-associated soil organic carbon: Implications for C sequestration in agricultural soils. Sci. Total Environ. 772, 145037. https://doi.org/10.1016/j.scitotenv.2021.145037.

Wang, F.M., Sanders, C.J., Santos, I.R., Tang, J.W., Schuerch, M., Kirwan, M.L., Kopp, R.E., Zhu, K., Li, X.Z., Yuan, J.C., Liu, W.Z., Li, Z.A., 2021a. Global blue carbon accumulation in tidal wetlands increases with climate change. Nat. Sci. Rev. 8(9), nwaa296. https://doi.org/10.1093/nsr/nwaa296.

Wang, S.M., Jia, Y.F., Liu, T., Wang, Y.Y., Liu, Z.G., Feng, X.J., 2021b. Delineating the Role of calcium in the large-scale distribution of metal-bound organic carbon in soils. Geophys. Res. Lett. 48, e2021GL092391. https://doi.org/10.1029/2021GL092391.

Wang, W.Q., Sardans, J., Wang, C., Zeng, C.S., Tong, C., Chen, G.X., Huang, J.F., Pan, H.R., Peguero, G., Vallicrosa, H., Peñuelas, J., 2019. The response of stocks of C, N, and P to plant invasion in the coastal wetlands of China. Global Change Biol. 25(2), 733–743. https://doi.org/10.1111/gcb.14491.

Wang, Z.H., Zhang, J.Y., Yang, X.M., Huang, C., Su, F.Z., Liu, X.L., Liu, Y.M., Zhang, Y.Z., 2022. Global mapping of the landside clustering of aquaculture ponds from dense time-series 10 m Sentinel-2 images on Google Earth Engine. Int. J. Appl. Earth OBS. 115, 103100. https://doi.org/10.1016/j.jag.2022.103100.

Wei, Z.Q., Ji, J.H., Li, Z., Yan, X., 2017. Changes in organic carbon content and its physical and chemical distribution in paddy soils cultivated under different fertilisation practices. J. Soil. Sediment. 17, 2011–2018. https://doi.org/10.1007/s11368-017-1676-6.

Were, D., Kansiime, F., Fetahi, T., Cooper, A., Jjuuko, C., 2019. Carbon sequestration by wetlands: a critical review of enhancement measures for climate change mitigation. Earth Syst. Environ. 3, 327–340. https://doi.org/10.1007/s41748-019-00094-0.

Xia, S.P., Wang, W.Q., Song, Z.L., Kuzyakov, Y., Guo, L.D., Zwieten, L.V., Li, Q., Hartley, L.P., Yang, Y.H., Wang, Y.D., Qunie, T.A., Liu, C.Q., Wang, H.L., 2021. *Spartina alterniflora* invasion controls organic carbon stocks in coastal marsh and mangrove soils across tropics and subtropics. Global Change Biol. 27, 1627–1644. https://doi.org/10.1111/gcb.15516.

Xie, R.R., Zhu, Y.C., Li, J.B., Liang, Q.Q., 2019. Changes in sediment nutrients following *Spartina alterniflora* invasion in a subtropical estuarine wetland, China. Catena 180, 16–23. https://doi.org/10.1016/j.catena.2019.04.016.

Xu, J.M., Yuan, K.N., 1993. Dissolution and fractionation of calcium-bound and iron- and aluminum-bound humus in soils. Pedosphere 3, 75–80.

Yang, P., Zhang, L.H., Lai, D.Y.F., Yang, H., Tan, L.S., Luo, L.J., Tong, C., Hong, Y., Zhu, W.Y., Tang, K.W., 2022a. Landscape change affects soil organic carbon mineralization and greenhouse gas production in coastal wetlands. Global Biogeochem. Cy. 36, e2022GB007469. https://doi.org/10.1029/2022GB007469.

Yang, P., Tang, K.W., Yang, H., Tong, C., Yang, N., Lai, D.Y.F., Hong, Y., Ruan, M.J., Tan, Y.Y., Zhao, G.H., Li, L., Tang, C., 2022b. Insights into the farming-season carbon budget of coastal earthen aquaculture ponds in southeastern China. Agr. Ecosyst. Environ. 335, 107995. https://doi.org/10.1016/j.agee.2022.107995.

Yang, P., Tang, K.W., Zhang, L., Lin, X., Yang, H., Tong, C., Hong, Y., Tan, L.S., Lai, D.Y.F., Tian, Y.L., Zhu, W.Y., Ruan, M.J., Lin, Y.X., 2023. Effects of landscape modification on coastal sediment nitrogen availability, microbial functional gene abundances and N_2O production potential across the tropical-subtropical gradient. Environ. Res. 227, 115829. https://doi.org/10.1016/j.envres.2023.115829.

Ye, C.L., Bai, T.S., Yang, Y., Zhang, H., Guo, H., Li, Z., Lin, H.X., Hu, S.J., 2017. Physical access for residue-mineral interactions controls organic carbon retention in an Oxisol soil. Sci. Rep. 7(1), 6317. https://doi.org/10.1038/s41598-017-06654-6.

Yeasmin, S., Singh, B., Johnston, C.T., Sparks, D.L., 2017. Organic carbon characteristics in density fractions of soils with contrasting mineralogies. Geochimi. Cosmochim. Ac. 218, 215–236. http://dx.doi.org/10.1016/j.gca.2017.09.007.

Yu, C.X., Xie, S.R., Song, Z.L., Xia, S.P., Åström, M.E., 2021. Biogeochemical cycling of iron (hydr-)oxides and its impact on organic carbon turnover in coastal wetlands: a global synthesis and perspective. Earth-Sci. Rev. 218, 103658. https://doi.org/10.1016/j.earscirev.2021.103658.

Yu, M.X., Wang, Y.P., Jiang, J.J., Wang, C., Zhou, G.Y., Yan, J.H., 2019. Soil organic carbon stabilization in the three subtropical forests: Importance of clay and metal oxides. J. Geophys. Res-Biogeo. , 124. https://doi.org/10.1029/2018JG004995.

Zhao, B., Dou, A., Zhang, Z.W., Chen, Z.Y., Sun, W.B., Feng, Y.L., Wang, X.J., Wang, Q., 2023. Ecosystem-specific patterns and drivers of global reactive iron mineral-associated organic carbon. Biogeosciences 20, 4761–4774. https://doi.org/10.5194/bg-20-4761-2023.

Zhang, X.H., Zhang, Z.S., Li, Z., Li, M., Wu, H.T., Jiang, M., 2021. Impacts of *Spartina alterniflora* invasion on soil carbon contents and stability in the Yellow River Delta, China. Sci. Total Environ. 775, 145188 https://doi.org/10.1016/j.scitotenv.2021.145188.

Zhong, Z.K., Han, X.H., Xu, Y.D., Zhang, W., Fu, S.Y., Liu, W.C., Ren, C.J., Yang, G.H., Ren, G.X., 2019. Effects of land use change on organic carbon dynamics associated with soil aggregate fractions on the Loess Plateau, China. Land Degrad. Dev. 30, 1070–1082. http://dx.doi.org/10.1002/ldr.3294.

Zhu, Y.S., Wang, Y.D., Guo, C.C., Xue, D.M., Li, J., Chen, Q., Song, Z.L., Lou, Y.L., Kuzyakov, Y., Wang, Z.L., Jones, D.L., 2020. Conversion of coastal marshes to croplands decreases organic carbon but increases inorganic carbon in saline soils. Land Degrad. Dev. 31, 1099–1109. https://doi.org/10.1002/ldr.3538.

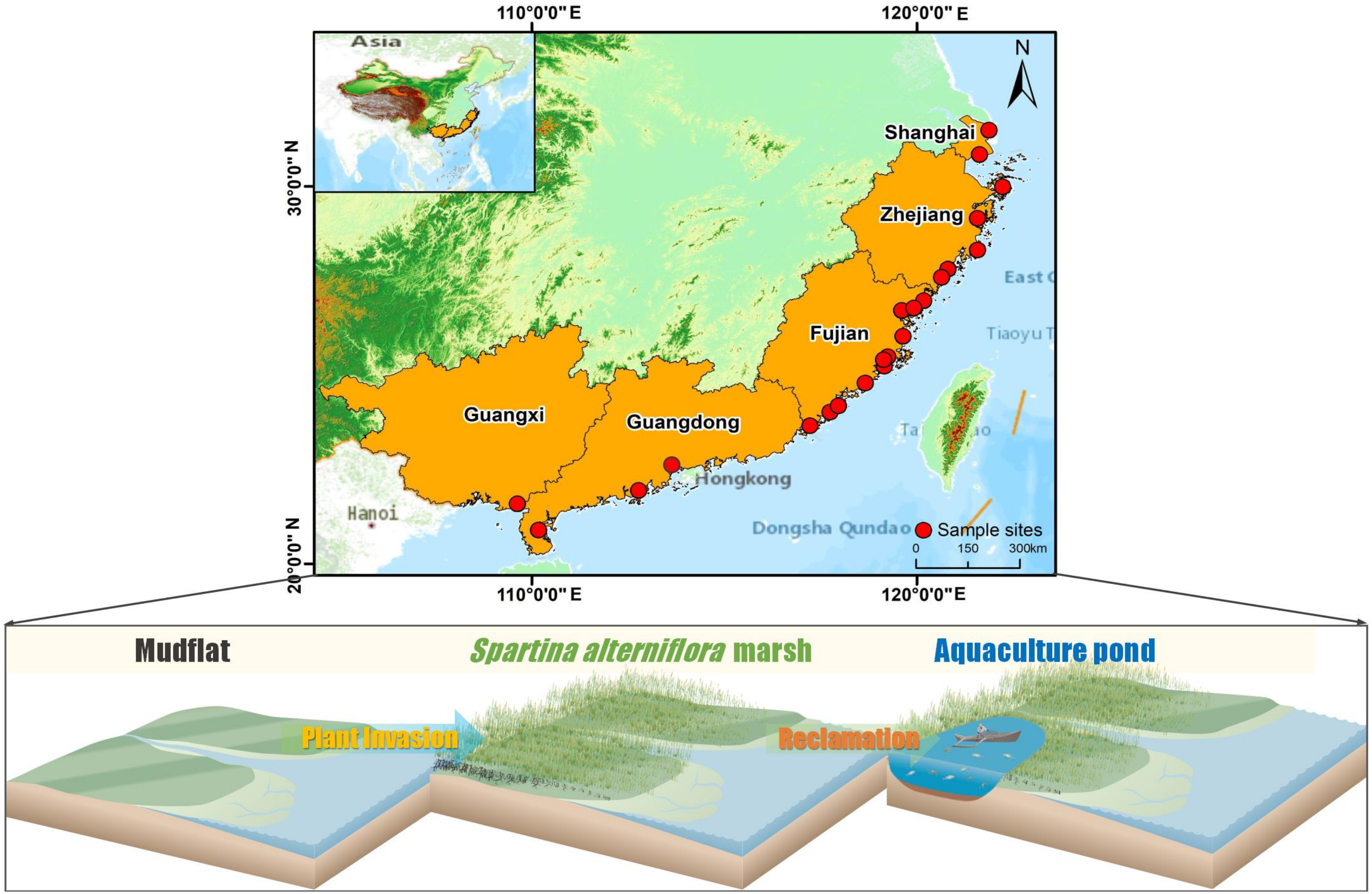

FIGURE 1 Locations of the 21 coastal wetlands in southeastern China. Three habitat types were investigated at each wetland including mudflat, *S. alterniflora* marshes and aquaculture ponds.

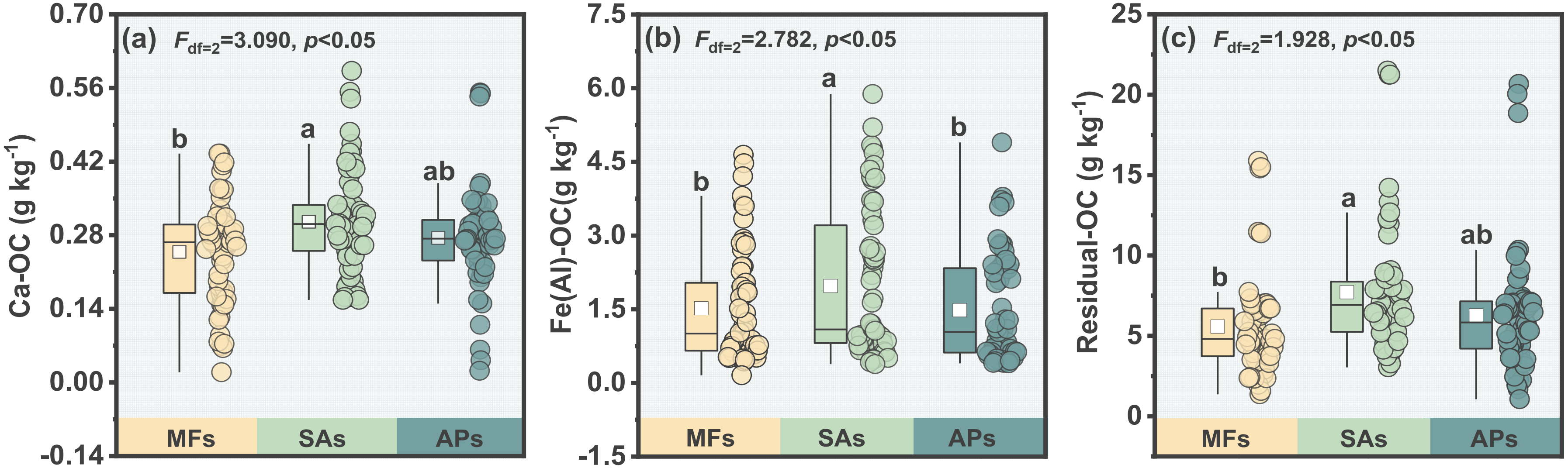

FIGURE 2 Box plots of (a) Ca-OC, (b) Fe(Al)-OC and (c) residual-OC contents in the top soil (0–20 cm) of mud flats (MFs), *S. alterniflora* marshes (SAs) and aquaculture ponds (APs) in coastal wetlands in southeastern China (n = 63). Bars with no overlapping letters are significantly different (p<0.05).

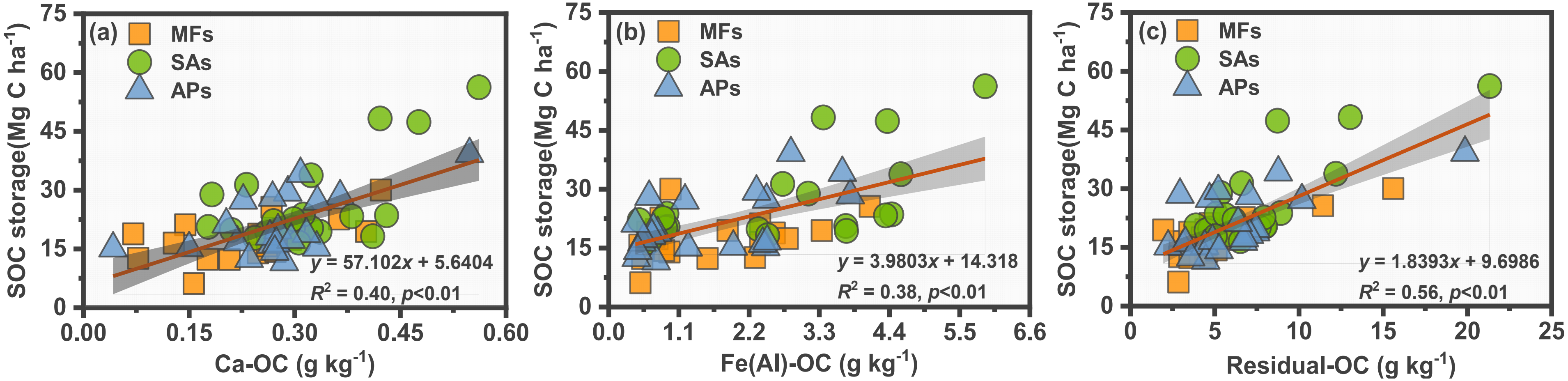

FIGURE 3 Linear regression between SOC storage and (a) Ca-OC, (b) Fe(Al)-OC, and (c) residual-OC contents in the top soil (0–20 cm) of all sampling sites. MFs, SAs and APs represent mud flats, *S. alterniflora* marshes and aquaculture ponds, respectively.

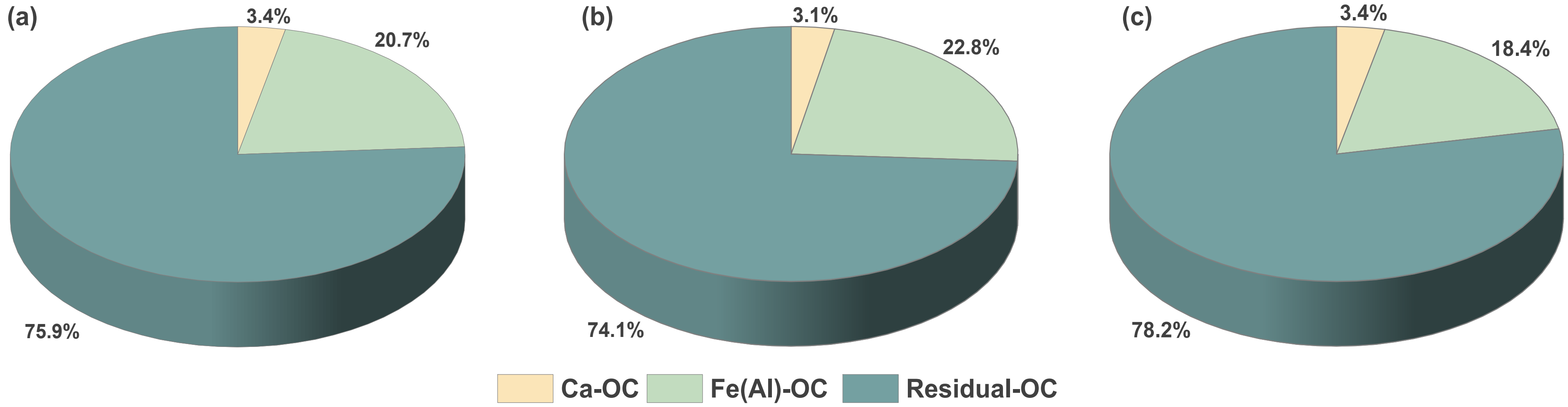

FIGURE 4 Proportions of mineral-bound and residual organic carbon contents in the top soil (0–20 cm) of (a) mudflats, (b) *S. alterniflora* marshes, and (c) aquaculture ponds in coastal wetlands in southeastern China.

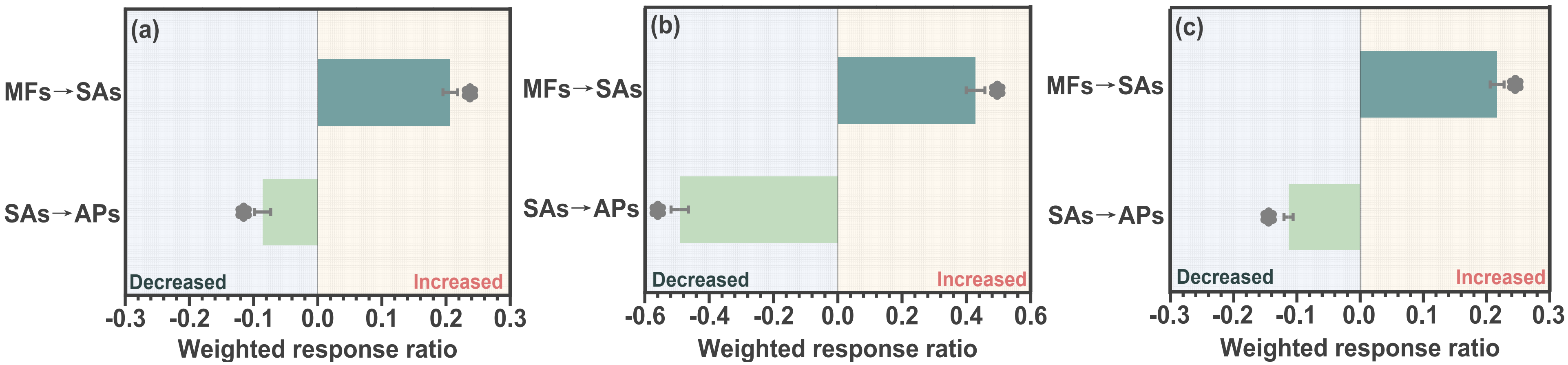

FIGURE 5 Weighted response ratios (RR++) of (a) Ca-OC, (b) Fe(Al)-OC, and (c) residual-OC contents for the different land cover change scenarios: MFs→SAs represents transformation from mudflats to *S. alterniflora* marshes; SAs→APs represents conversion from *S. alterniflora* marshes to aquaculture ponds. Bars represent the RR++ values and 95% CIs (n = 21 sampling sites). The asterisks (*) indicate significant differences at $p < 0.05$.

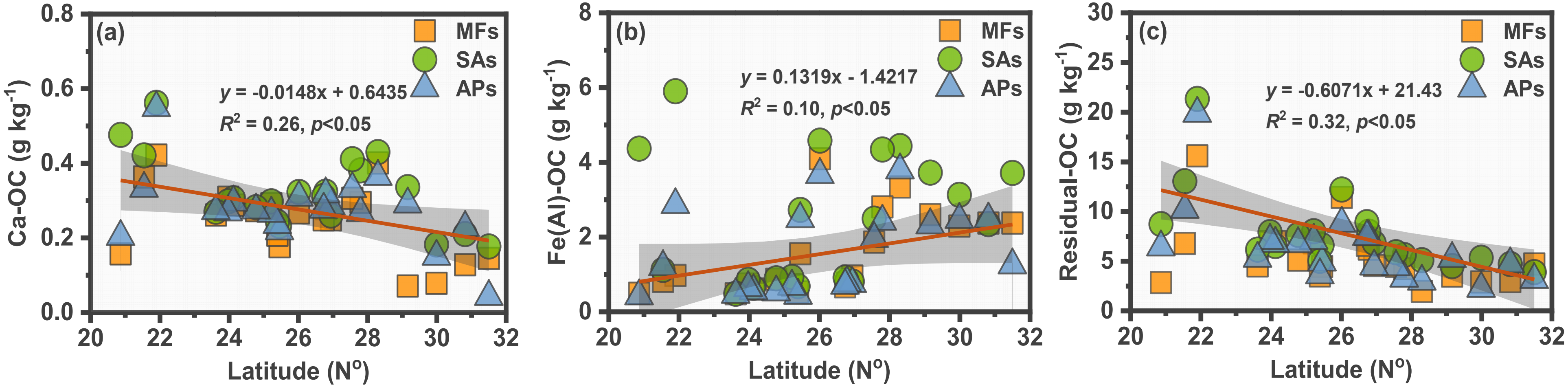

19

20 **FIGURE 6** Linear regressions between latitude and (a) Ca-OC, (b) Fe(Al)-OC, and (c) residual-OC contents in the top soil (0–20 cm) across

21 all sample sites. MFs, SAs and APs represent mud flats, *S. alterniflora* marshes and aquaculture ponds, respectively.

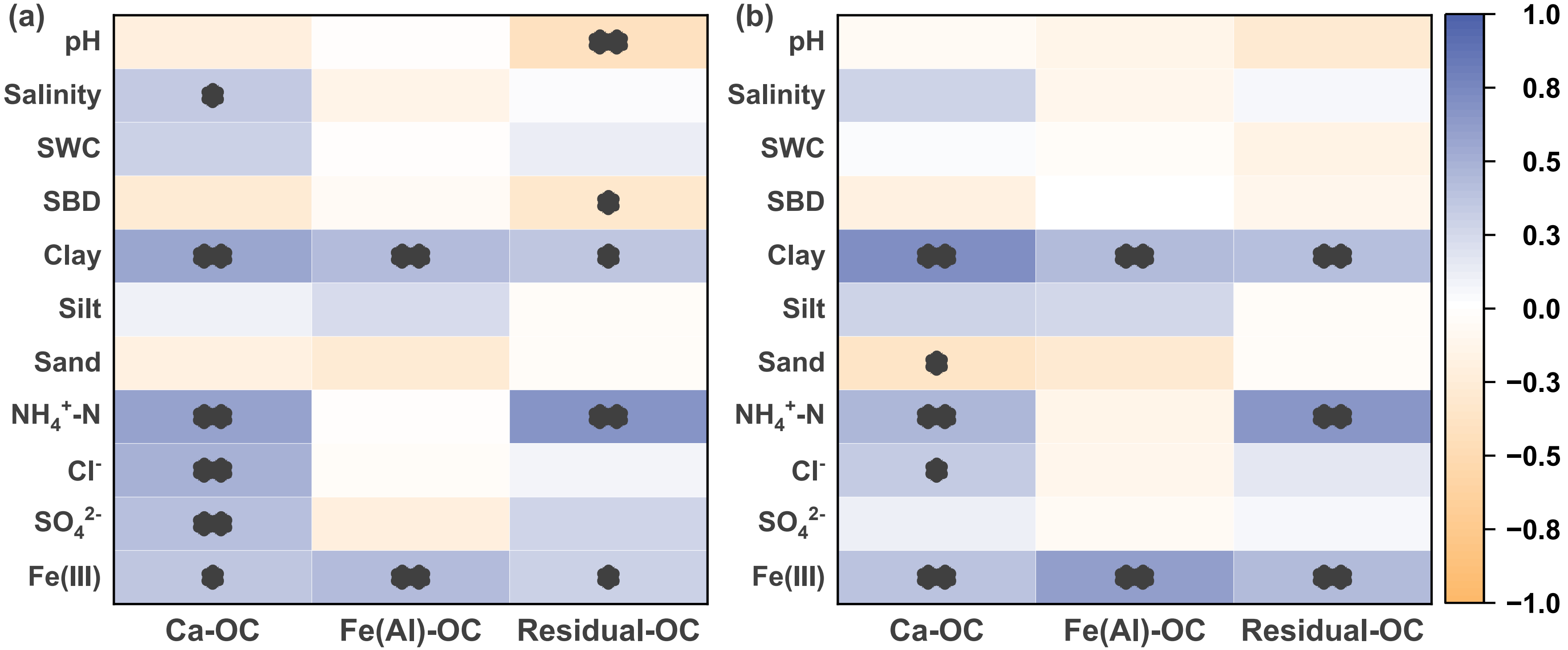

FIGURE 7 Correlation coefficients between Ca-OC, Fe(Al)-OC, residual-OC and different soil physicochemical variables in surface soil (0–20 cm) for the different land cover change scenarios: (a) Transformation of mudflats to *S. alterniflora* marshes; (b) Conversion of *S. alterniflora* marshes to aquaculture ponds. Colors of the rectangular segments indicate the direction and strength of correlation (blue = positive; orange = negative; r = –1 to 1); asterisks indicate levels of significance (*p <0.05; **p < 0.01). See main text for explanation of abbreviations.

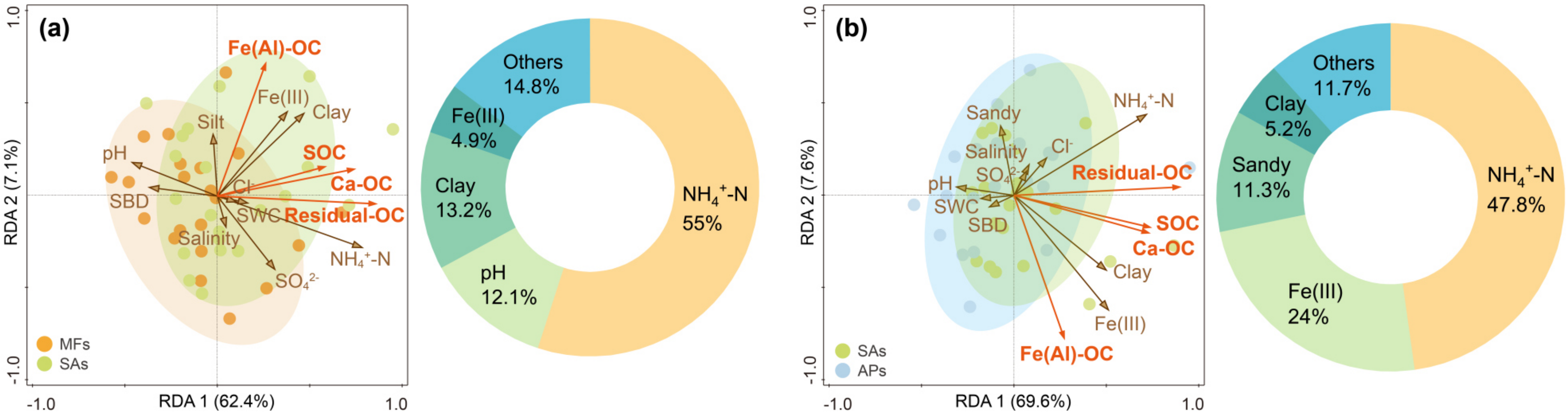

FIGURE 8 Redundancy analysis (RDA) biplots of the relationships between Ca-OC, Fe(Al)-OC, residual-OC and various physicochemical variables in surface soil (0–20 cm) for the different land cover change scenarios: (a) Transformation of mudflats to *S. alterniflora* marshes; (b) Conversion of *S. alterniflora* marshes to aquaculture ponds. The pie charts show the percentages of variance in Ca-OC, Fe(Al)-OC and residual-OC explained by the different variables. See main text for explanation of abbreviations.

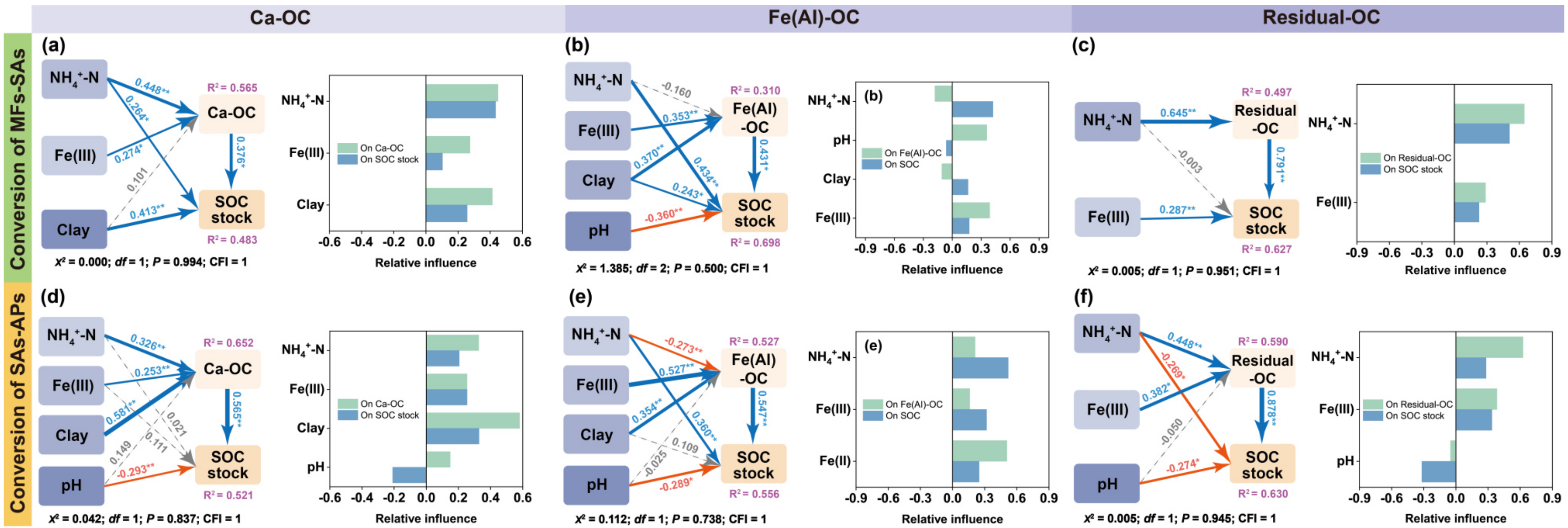

FIGURE 9 Partial least square structural equation modeling (PLS-SEM) to evaluate the direct and indirect effects of soil physicochemical variables on Ca-OC, Fe(Al)-OC, residual-OC and SOC under different land cover change scenarios: (a-c) Transformation of mudflats to *S. alterniflora* marshes; (d-f) Conversion of *S. alterniflora* marshes to aquaculture ponds. Solid blue and red arrows indicate significant positive and negative effects, respectively, and dashed arrows indicate insignificant effect on the dependent variables. Numbers adjacent to arrows are standardized path coefficients, indicating the effect size of the relationship. R^2 represents the variance explained for target variables. Asterisks indicate levels of significance (*$p < 0.05$; **$p < 0.01$).

Supporting Information

Variable responses of mineral-bound soil organic carbon to land cover change in coastal wetlands, southern China

Ping Yang[a,b,c], Guanpeng Chen[a], Linhai Zhang[a,c*], Chuan Tong[a,c], Hong Yang[d,e], Wanyi Zhu[a], Dongyao Sun[f*], Lishan Tan[g], Yan Hong[a], Kam W. Tang[h*]

[a]*School of Geographical Sciences, Fujian Normal University, Fuzhou 350117, P.R. China,*

[b]*Institute of Geography, Fujian Normal University, Fuzhou 350117, China*

[c]*Research Centre of Wetlands in Subtropical Region, Fujian Normal University, Fuzhou 350117, P.R. China*

[d]*Department of Geography and Environmental Science, University of Reading, Reading, UK*

[e]*College of Environmental Science and Engineering, Fujian Normal University, Fuzhou 350007, China*

[f]*School of Geography Science and Geomatics Engineering, Suzhou University of Science and Technology, Suzhou 215009, China*

[g]*Department of Geography and Resource Management, The Chinese University of Hong Kong, Shatin, New Territories, Hong Kong SAR, China*

[h]*Department of Biosciences, Swansea University, Swansea SA2 8PP, U. K.*

***Correspondence to:**

Linhai Zhang (mary12maryzhang@126.com); Dongyao Sun (dongyaos@126.com); Kam W. Tang (k.w.tang@swansea.ac.uk)

Telephone: 086-0591-87445659 **Fax:** 086-0591-83465397

Supporting Information Summary

No. of pages: 7 **No. of figures:** 3 **No. of tables:** 2

Page S3: Figure S1 Linear regression between latitude and mean annual air temperature.

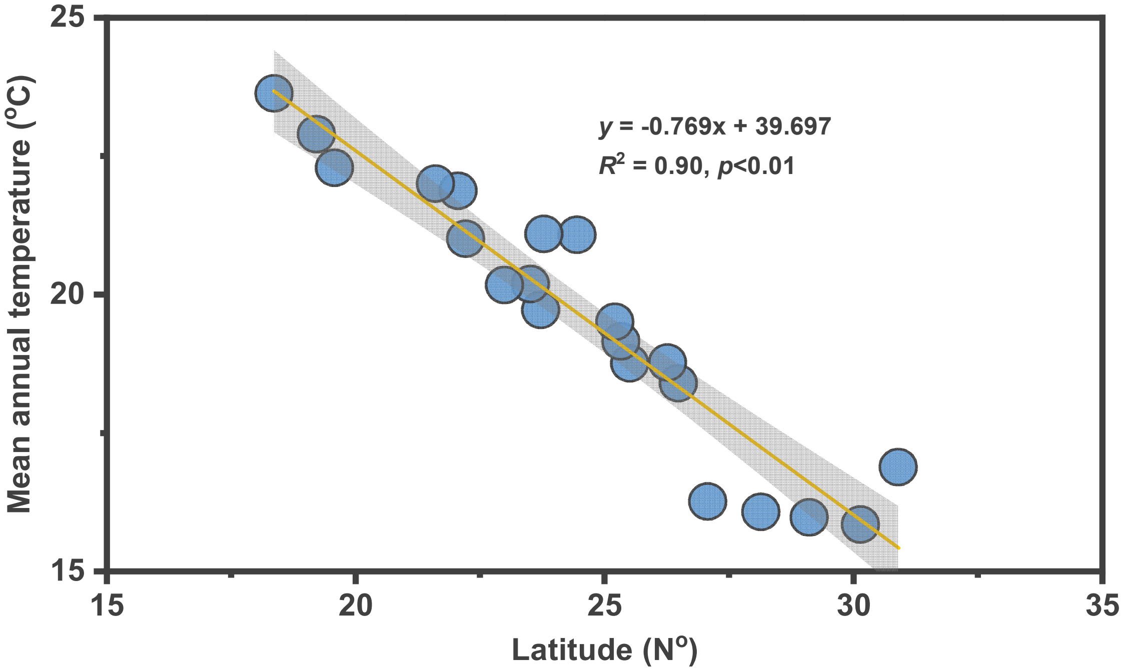

Figure S1 Linear regression between latitude and mean annual air temperature.